한국도시방재학회논문집
창간호 제1호 2001년 6월
pp. 117~125

비활성 그리고 활성 단층지역 내부와 주변에서의 응력장에 대한 수치적 분석

Numerical Analysis of Stress Regimes in and around Inactive and Active Fault Zones

정 우 창* · 송 재 우**
Jeong, Woo-Chang · Song, Jai-Woo

Abstract

This paper presented the analysis of stress regimes in and around inactive and active fault zones. The stress regime in the vicinity of an existing inactive fault zone is dependent on the orientation of the fault with respect to the current stress field and the contrast between the elastic properties of the faulted rock and those of the surrounding rock. In the analysis of stress regimes around an active fault zone, if the yielding stress is exceeded during loading, the localized shearing in a fault zone will result in weakness with mean stresses in the fault becoming lower than those in the surrounding rock. It can be expected that such stress gradients will induce fluid flow towards the faults zone.

Keywords : stress regime, fault zones, stress gradient, Mohr-Coulomb plasticity

요 지

비활성 그리고 활성 단층지역의 내부와 주변에서 발생하는 응력장의 변화에 대한 수치적 분석이 수행되었다. 존재하는 비활성 단층지역 근처에서의 응력장은 단층의 방향과 단층화된 암반과 주위의 비단층화된 암반의 탄성적 특성 사이의 대조에 따라 변화한다. 활성 단층지역 주위의 응력장에 대한 분석에서, 만약 단층지역의 항복응력이 초과된다면, 단층지역 내에서의 국부화된 전단응력은 주위의 비단층화된 암반에서의 평균응력 보다 작게 되는 단층 내에서의 평균응력의 감소를 유발시킨다. 따라서 이러한 응력경사는 단층지역내로 유체의 흐름을 기대할 수 있다.

핵심용어 : 응력장, 단층지역, 응력경사, Mohr-Coulomb 소성

* Member, Researcher, Center of Disaster Prevention and Safety Management, Hong-Ik University
** Member, Professor, Department of Civil Engineering, Hong-Ik University

1. Introduction

The hydrogeological behavior of faults is a key area of uncertainty in understanding groundwater flow and radionuclide transport in the vicinity of deep repositories for radioactive waste. Predictions of radionuclide movement in a faulted host rock require an understanding of the hydraulic of the structure of potential fluid flow and transport paths along faults, as well as an understanding of the hydraulic significance of faults in the context of the regional flow field. It is also important to consider the potential for changes in fault hydrogeology resulting from fault reactivation in evolving stress fields. Evolution of stress and fluid pressure fields can result in fault reactivation, which may induce a hydraulic response in the vicinity of the fault and may lead to changes in the hydrogeology of the fault.

In the numerical approaches to account for the effects of stress evolution, porous medium and fractured network treat the solid matrix as a rigid material or as a material having an elastic rheology. For example, the effects of large ice loads during glacial periods were considered in a study by SKI (1991), using the three-dimensional distinct element code, 3DEC. Additionally, the effects of loading, melting and unloading on a geological system containing a number of fracture zones were examined. Models results indicated that stress changes are relieved through small movements in major fault zones. However, the model did not include hydromechanical effects and the potential for fault movements to alter hydraulic conductivity in the fault zone. A similar approach was taken by HMIP (1992) in an analysis of rock mass response to glaciation in the Dounreay area in Scotland. Application of the 3DEC model revealed displacements on faults of the order of 1 meter. Muir-Wood and King (1993) considered only uniform loading and did not resolve variations in stress within fault zones in their model of fluid flow in pressurized cracks, developed to explain hydrological phenomena connected with earthquakes. Sibson (1994) considered the dynamic effects of differential stress in the vicinity of faults, including the formation of pressure gradients, but did not model the internal properties of fault zones. Such treatments of faults may not adequately explain porosity and fluid pressure variations or phenomena such as pressure solution creep (Rutter, 1976), grain size reduction, and fault sealing mechanisms, which may be better described by elastoplastic or viscous fault rheologies.

The aim of this study is to evaluate the magnitude of stresses generated in the vicinity of fault zones in response to stress loading. Plastic behavior is assumed when yielding stresses are attained. Irreversible deformation of the solid is modeled for situations in which the fault zone and surrounding rock have distinct material

properties. Two phases have been considered in this paper: 1) stress regimes in the vicinity of inactive fault zones, and 2) stress regimes in the vicinity of active faults.

2. Stress Regimes around Inactive and Active Fault Zones

2.1 Stress Regimes around Inactive Fault Zones

These stress regimes generated in response to homogeneous loading, have been evaluated by assuming an elastic rheology to describe the material properties of the fault zone and surrounding rock matrix. An elastic rheology is considered appropriate for an inactive fault zone because yielding stresses are not achieved. Gradients in stress are generated during loading both within and outside the fault zone because the fault zone and the surrounding rock have contrasting elastic properties. This analysis was carried out using the ANSYS rock mechanics model (Kohnke, 1987).

Many investigations have observed distinct changes in stress patterns either side of fault zones (for example, stress variations in the vicinity of a fault in the Lac du Bonnet Batholith in Canada, Stevenson et al., 1996a,b). As stress and train patterns develop during phases of stress loading and unloading, they can affect permeability and porosity distributions around the fault, and thus induce groundwater flow transients. An initial study was undertaken to examine the relationship between faults and local stress distributions.

For this analysis, fault zones were assumed to be existing zones of weakness with simple geometries and characteristic rheologies that differ from that of the surrounding rock. Stress regimes were evaluated assuming a linear elastic behavior for the fault zone and surrounding rock. Wedge-shaped fault geometry was assumed on the basis that fault zones would evolve naturally (growing or bending) to accommodate any local stress concentrations associated with irregularities in geometry (Fig. 1).

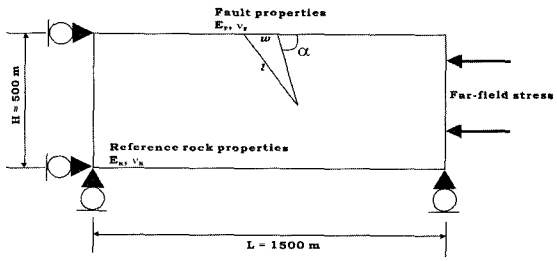

Fig. 1 Conceptual Model for Calculation of Stress Fields in the Vicinity of Inactive Faults

Stress and strain distributions were determined by solving the equation of equilibrium coupled with constitutive laws for linear elastic solid. Using tensor notation, the equilibrium equations may be expressed as follows:

$$\frac{\partial \sigma_{ij}}{\partial x_j} + \rho g_i = 0 \quad (1)$$

where σ_{ij} are the stresses (Pa), ρ is the solid density ($Kg\ m^{-3}$), g_i are the components of gravitational acceleration ($m\ s^{-3}$), and x_j are distances (m). The strains are given by:

$$\varepsilon_{ij} = \frac{1}{2}\left[\frac{\partial u_i}{\partial x_i} + \frac{\partial u_j}{\partial x_i}\right] \quad (2)$$

where u_i are the displacements (m) and the stress-strain relations are:

$$\sigma_{ij} = \delta_{ij}\left[\frac{Ev}{(1+v)(1-2v)}\varepsilon_{kk}\right] + \frac{E}{(1+v)}\varepsilon_{ij} \quad (3)$$

where E is Young' s modulus (Pa) and v is Posson' s ratio.

These equations were solved in two dimensions (assuming plane stress conditions) using the finite element code ANSYS single fault zone were modeled to determine the range of stress distributions in response to stress loads. A modeling domain of length 1500 m was assumed and far-field stresses were applied at the boundaries, as shown in Fig. 1.

The spatial resolution of the finite element mesh in the fault zones was 1m. Values for the elastic properties of the fault (Young' s modulus and Poisson' s ratio) and other model parameters are given in Table1.

The mean stress distribution, σ_m=0.5 [σ_1 +σ_3] where σ_1 and σ_3 are the maximum and minimum principal stresses, was computed in the vicinity of faults for different fault geometries. Tensile and compressive loads of 10 MPa (typical stresses in stable regions at likely repository depths) were

Table 1. Fault Zone Modeling Parameters

Parameter	Symbol	Value
Model geometry		
Length	L	1500 m
Depth	H	500 m
Rock properties		
Poisson' s ratio	v_R	0.25
Young' s modulus	E_R	10 GPa
Fault geometry		
Width at surface	W	25 to 50 m
Dip	α	30° to 60°
Length	$l\ (\alpha = 30°)$	250 to 500 m
	$l\ (a = 60°)$	144 to 288 m
Fault rock properties		
Poisson' s ratio	v_F	0.2 to 0.4
Young' s modulus	E_F	0.05 $E_R$to 0.5 E_R
Boundary stress		
Far-field stress	$\Delta\sigma_{compressive}$	10 MPa
	$\Delta\sigma_{tensile}$	10 MPa

applied at a vertical model boundary.

First, the mean stress pattern in the vicinity of a fault was evaluated for different fault dips (30° and 60°), with other parameters fixed (l = 250 m, w = 25 m, ν_F = 0.4 and E_F/E_R = 0.5). For tensile deviatoric loads applied to a fault dipping at 30°, the mean stresses inside the fault were predicted to be higher than those in the footwall and hanging wall. Near the fault, the stress field in the rock mass rotated such that the minimum principal stresses were approximately parallel to the fault and the maximum principal stresses were normal to the fault. Numerical results are shown in Fig. 2 for the central region of the model containing the fault. For a fault dipping at 60°, the mean stresses inside the fault were shown to be lower than those in the surrounding rocks. In this case, the stress field in the rock mass near the fault rotated such that the minimum principal stresses were normal to the fault and the maximum principal stresses were parallel to the fault.

Second, the significance of fault length was investigated (l = 250 m and 500 m) for a fault subjected to tensile loads, with other parameters fixed (w = 25 m, α = 30°, ν_F = 0.4 and E_F/E_R = 0.5). The pattern of induced stress in and around the fault was shown to be insensitive to fault length. Similarly, changes to fault width (w = 25 m and 50 m) had little effect on the induced stress distribution (l = 25 m, α = 30°, ν_F = 0.4 and E_F/E_R = 0.5).

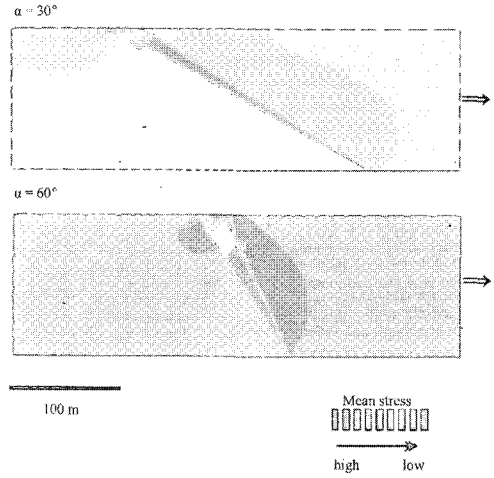

Fig. 2 Stress Pattern Around Faults of Different Dip Subjected to Tensile Loads.

Finally, the significance of the elastic properties was studied. The contrast in Young's modulus between the fault and the surrounding rock was investigated by comparing the results for E_F/E_R = 0.05 with those for E_F/E_R = 0.5 for tensile induced stresses. Other parameters were fixed at w = 50 m, l = 250 m, α = 30° and ν_F = 0.4. The contrast in induced mean stress between the fault zone and the surrounding rock was greatest for the case in which E_F/E_R = 0.5. The mean stress pattern was also predicted to be sensitive to the Poisson's ratio of the fault. Results were compared for ν_F = 0.2 and ν_F = 0.4, with α = 60°, E_F/E_R = 0.5, w = 50 m and l = 250 m. Higher mean stresses were predicted inside the fault for the case with a smaller Poisson's ratio.

The results confirm that faults can influence

the distribution of induced stress in response to loading. During such phases, induced gradients in stress and strain may initiate fluid flow transients. Significant factors influencing the form of the induced stress field in the vicinity of the fault are the contrast in elastic properties of the fault rock and surrounding rock, and the fault dip. Extensional stress changes, high fault dip ($\alpha = 60^{o}$), high Poisson' s ratio in the fault ($\nu_F = 0.4$) and small contrasts in Young' s modulus between bedrock and fault rock ($E_F/E_R = 0.5$) resulted in a reduction in mean stress inside the fault, which could induce fluid flow towards the fault zone.

2.2 Stress Regimes around Active Fault Zones

These stress regimes were generated in response to homogeneous loading and have been evaluated by assuming an elastoplastic rhelogy. Active deformation within the fault zone is represented by non-associated Mohr-Coulomb plasticity, allowing the progressive development of permanent strains within the fault zone to be modeled. Thus, stresses evolve at different rates within and outside the fault zone. This analysis was undertaken using FLAC rock deformation model (Cundall, 1989).

As stress is increased across a rock mass with elastic properties, a threshold is passed and failure or faulting is initiated along a localized zone of deformation. Yielding of brittle rocks may be described by non-associated Mohr-Coulomb plasticity, *i.e.*, plasticity independent of the stress failure surface (Mandl, 1988). For such problems, the equations of motion may be expressed as:

$$\frac{\partial \sigma_{ij}}{\partial x_j} + \rho g_i = \rho \frac{\partial^2 u_i}{\partial t^2} \tag{4}$$

where t is time (s) and a yielding function $f(Pa)$ based on the Mohr-Coulomb failure criterion may be defined as:

$$f = \frac{1}{2}(\sigma_3 - \sigma_1) + \frac{1}{2}(\sigma_3 + \sigma_1)\sin\phi' \; c\cos\phi' \tag{5}$$

where σ_i are the principal stresses, ϕ' is the friction angle and c is the cohesion (Pa). Yielding and plastic deformation occurs when $f = 0$ and $\partial f / \partial t = 0$ and increments in total strain are given by:

$$\Delta\varepsilon_i = \Delta\varepsilon_i^e + \Delta\varepsilon_i^p \tag{6}$$

where ε^e is elastic strain and ε^π is plastic strain, and their components are coaxial with the principal stresses. The plastic strain is calculated according to the flow rule:

$$\Delta\varepsilon_i^p = \lambda \frac{\partial G}{\partial \sigma_i} \tag{7}$$

where G is the plastic potential (Pa) given by:

$$G = \frac{1}{2}(\sigma_3 - \sigma_1) + \frac{1}{2}(\sigma_3 + \sigma_1)\sin\psi - c\cos\psi \tag{8}$$

and Ψ is the dilation angle.

Vermeer (1990) provided a theoretical insight into the implications of the Mohr-Coulomb plasticity model for stress field development during shear band formation in soil samples. The Mohr-Coulomb model predicts that the rate of change of stress within the plane of a shear band and parallel to the direction of shearing is less than the rate of changes of stress in the same direction outside the shear band. Vermeer (1990) calculated stress ratios of about 0.6 developing across shear bands, and reported that a suction is generated around shear bands in biaxial tests on soil samples which can be attributed to such induced stress discontinuities. The stress discontinuity is accompanied by softening (*i.e.*, a reduction in the major compressive stress that is causing shear). Vermeer (1990) calculated stress drops of about 10% of the yield value for shear bands induced at an angle of about 30° degrees to the loading direction.

Thus, the Mohr-Coulomb model can be expected to predict strain localization in an active fault accompanied by a decrease in fluid pressure in the fault. This strain localization mechanism is capable of explaining the initiation of a new fault, oriented according to the loading direction and potentially cutting pre-existing heterogeneities in the rock mass. The process does not require a pre-existing zone of weakness in the rock.

Numerical simulations have been conducted for various tectonic settings

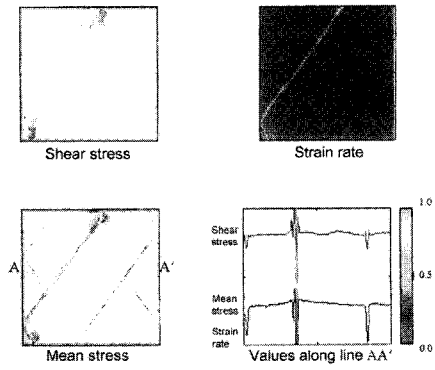

Fig.3 FLAC Illustration of the Mean Stress Reduction Resulting from Localized Shearing in a Mohr-Coulomb Material.

using the finite-difference code FLAC (Cundall, 1989) to solve eqns. (4)~(8) under plane strain conditions. In these simulations, the initiation of active faulting and the positions of the faults are not defined *a priori*. Several localized deformation zones with differing orientations may be initiated during a single simulation, and mean stress is always lower within these zones than in the surrounding rock, irrespective of the stress regime and the complexity of the fault system. Results from an example calculation of the development of a series of strike-slip faults on a 400 X 400 node horizontal grid are shown in Fig. 3. In this case, the friction angle and the dilation angle are 30° and 0° respectively. Opposing constant compressional velocities have been applied to the upper and lower boundaries of the problem shown in Fig. 3, with the other two boundaries at fixed

stress. The diagram shows that one fault is currently active in the stress regime, and that the mean stresses are lower where localized shearing has occurred.

3. Summary and Conclusions

This paper presented an analysis of the stress regimes that may occur in the vicinity of fault zones and has considered the hydraulic effects of localized strain during active faulting. The analysis of active faults differs from many previous studies in that irreversible deformation of the solid and stress discontinuities between the fault and surrounding rock have been considered. The analysis has led to the following conclusions:

1) The stress regime around an existing fault zone is dependent on the orientation of the fault with respect to the current stress field, and the contrast between the elastic properties of the faulted rock and those of the surrounding rock. Extensional stress regimes, high fault dip, high Poisson' s ratio in the fault, and small contrasts in Young' s modulus between bedrock and faulted rock result in lower mean stresses inside the fault than outside the fault. Potentially, fluid flow towards the fault zone could be induced during the development of the stress field under such conditions.

2) If the yielding stress is exceeded during loading, the Mohr-Coulomb plasticity model predicts that localized shearing in a fault zone will result in softening with mean stresses in the fault becoming lower than those in the surrounding rock. Such stress gradients will induce fluid flow towards the fault zone. The magnitude of the stress difference increases with depth, which implies that flow would be oriented toward the lower regions of the active part of a fault.

References

1. SKI(1991), SKI-Project-90, SKI Technical Report 91:23, SKI, Stockholm, Sweden.
2. HMIP(1992), " Modeling of Rock Mass Response to Glaciation in the Dounreay Area" , Scotland, DOE/HIMP Report.
3. Muir-Wood, R. and King, G.C.P.(1993), " Hydrological Signatures of Earthquake Strain" , Journal of Geophysical Research, 98, B11, pp. 22035-22068.
4. Rutter, E.H.(1976), " The Kinetics of Rock Deformation by Pressure Solution" , Phil. Trans. Royal Soc. London 283a, pp. 203-219.
5. Sibson, R.H.(1994), " Crustal Stress, Faulting and Fluid Flow, in Geofluids: Origin, Migration and Evolution of Fluids in Sedimentary Basins" , Edited by J. Parnell, Geol. Soc. Spec. Publ., London, 78, pp. 68-84.
6. Kohnke, P.(1987), " ANSYS Engineering Analysis System" , Theoretical Manual, Swanson Analysis System Inc., Houston,

Pennsylvania.
7. Cundall, P.A.(1989), " Numerical Experiments on Localization in Frictional Materials" , Ingenieur Archiv, 59, pp. 148-159.
8. Mandl, G.(1988), " Mechanics of Tectonic Faulting: Models and Basic Concepts" , Elsevier, Amsterdam.
9. Vermeer, P.A.(1990), " The Orientation of Shear Bands in Biaxial Tests" , Geotechnique, Vol. 40, No. 2, pp. 223-236.